Bibliographical reference

Silent Owl Flight: Comparative Acoustic Wind Tunnel Measurements on Prepared Wings, Thomas Geyer, Ennes Sarradj and Christoph Fritzsche, Acta Acustica **vol. 99** (Number 1), 2013, pp. 139-153

DOI
https://doi.org/10.3813/AAA.918598

ACTA ACUSTICA UNITED WITH ACUSTICA
Vol. 99 (2013) 139 – 153
DOI 10.3813/AAA.918598

Silent Owl Flight: Comparative Acoustic Wind Tunnel Measurements on Prepared Wings[1]

Thomas Geyer, Ennes Sarradj, Christoph Fritzsche*
Brandenburg University of Technology, 03046 Cottbus, Germany. thomas.geyer@tu-cottbus.de

Summary
The wings and feathers of most genera of owls show unique properties that are held responsible for the silent flight of the owls. This ability to fly silently has long been of interest for engineers, with the aim to transfer the basic noise reducing mechanisms to technical applications such as blades of fans and propellers. The present paper describes acoustic and aerodynamic wind tunnel measurements on prepared bird wings of different species, among them two silently flying species of owls, the barn owl (*Tyto alba*) and the tawny owl (*Strix aluco*). The different wings are characterized in the study as technical airfoils in terms of their acoustic and aerodynamic performance. The experiments took place in an aeroacoustic open jet wind tunnel using microphone array measurement technique and deconvolution beamforming algorithms. Simultaneously to the acoustic measurements, the aerodynamic forces of the wings were captured using a six-component balance. This study, which is a complementary study to the approach of performing flyover measurements on birds flying in gliding flight, further confirms experimentally that the silent owl flight is a consequence of the special wing and plumage adaptations of the owls and not a consequence of their lower flight speed only.
PACS no. 43.28.Ra

1. Introduction

Owls are commonly known to fly very quietly. This silent flight is required to enable their survival regarding the hunting habits of the owl: The owl sits on a perch or flies very slowly and at a low altitude. When the owl aurally locates prey (e.g. mice, voles and other small animals), it approaches silently and the prey does not hear the owl early enough to still have the time to escape. The silent flight therefore has two purposes: First, the owl's own noise must not disturb its ability to locate the prey and second, the prey must not hear the owl's approach in time to escape. Non-silently flying birds of prey, on the other hand, visually spot their prey and fly very fast so that the prey simply has no time to escape due to the high speed of approach.

1.1. The Special Feather Adaptations of Owls

In order to pursuit this specially adapted hunting habit, owls have developed certain adaptations that distinguishes them from other birds of prey, making them unique among the birds. Besides differences in wing shape and wing loading, this is the special feather structure of the owls, which was subject to several biological studies in the past. An early investigation on the microstructure of the feathers of birds, including owls, was done by Mascha [1] in 1904, who describes a comb-like shape of the outer barbs of the owl's primary feathers as well as the very long and soft endings of the distal barbules, called pennula, that lead to a velvet-like surface of the feathers. He even assumes that the peculiarities of the owl feathers are sound muffling devices. 30 years later, in 1934, Graham [2] designated the three mechanisms of the feathers and the plumage of owls that supposedly enable the silent flight: (1) a comb-like structure at the leading edge of the wings, (2) long and soft fringes at the trailing edge and (3) a downy upper surface of the feathers. He assumed that the third mechanism either serves to muffle the small reverberations of sound or that it helps the further retardation of the boundary layer initiated by the comb-like leading edge. Sick [3] examined the microstructure of a variety of feathers of different bird species, stating that the soft consistence of the feathers of owls, as a result of the long, upward-bent pennula, leads to a noise absorption during flight. Hertel [4] provided further information on the special properties of the owl feathers leading to the low noise generation, including detailed microscopy pictures of the hooks that form the leading edge comb and the inner and the outer vanes with the long, soft fringes. The most recent work on the feather structure of owls is the work by Bachmann [5]. He performed detailed anatomical, morphometrical and biomechanical measurements on the wings of barn owls (*Tyto alba*) and compared the results to those of the pigeon, representing the non-silently flying birds. Thereby, advanced

Received 24 May 2012,
accepted 31 October 2012.

* now with the Thuringian State Institut for Environment and Geology

[1] A prior version of this paper was presented as Paper 2230 at the 18th AIAA/CEAS Aeroacoustics Conference (33rd AIAA Aeroacoustics Conference), 04–06 June 2012, Colorado Springs, CO.

measurement techniques like three-dimensional surface scans, three-dimensional digitizing and computed tomography scanners (to allow for the reconstruction of internal structures such as bones, skin and feather rachises) were used. Noticeable differences between the feather structure of both species were identified, including the longer pennula and lesser radiates of the feathers of the owl.

This short overview of biological studies of owls shows that these species are indeed different from other birds regarding their wings and feathers. The question that arises is whether the reported silent flight of owls results from these unique adaptations or from their low speed of flight compared to other birds of prey.

1.2. The Silent Flight of Owls

The silent flight of the owl as an inspiration for technical applications has been subject to scientific research for a long time. Inspired by a qualitative comparison of the flight noise of a "common" owl and a non-silently flying tawny fishing owl (*Ketupa flavipes*), Graham [2] studied the wings and feathers of owls. As a result he identified the above-mentioned three mechanisms that are held responsible for the low noise generation. Thorpe and Griffin [6] additionally noticed the lack of ultrasonic components in the flapping flight noise of owls. One of the most detailed studies regarding the silent owl flight was done in 1971 by Kroeger *et al.* [7] and by Gruschka *et al.* [8], where the aim was to use the knowledge of the quieting mechanisms of the owl for the development of future quiet aircraft. They conducted flyover measurements on a Florida barred owl (*Strix varia alleni*) during the phase of gliding flight in a reverberation chamber using a single condenser microphone. It was found that the noise spectrum of the owl is shifted strongly towards low frequencies well into the range where it cannot be heard by its prey [7]. Kroeger *et al.* further described the aerodynamic performance of the owls as being very poor (for example in terms of the lift-to-drag-ratio of the owl compared to that of an albatross). Additionally, wind tunnel tests were performed on two wings during which the flow field around the wing and the motions of the wing or single wing parts were observed. However, no acoustic wind tunnel measurements were done. Neuhaus *et al.* [9] compared the flight noise of tawny owls (*Strix aluco*) and mallard ducks (*Anas platyrhynchos*), although the measurements were conducted under completely different conditions. They performed flyover measurements using a single microphone and a frequency analyzer and found that the owl's flight noise during gliding flight has a low frequency character that the duck's has not. It shows a peak of the sound pressure level between 200 Hz and 700 Hz, and it is stated that this low frequency noise is below the hearing limit of the typical prey of the tawny owl. Neuhaus *et al.* also did flow visualization experiments in a wind tunnel and observed "a much higher degree of laminar flow" around the owl wing than around the duck wing. Anderson [10] investigated the aerodynamic function of the comb-like structure at the wing leading edge. Revisiting the data of Kroeger *et al.* [7] he concludes that the comb acts as a high lift device as it delays the separation of the flow at higher angles of attack. Another study on the silent flight of owls was done by Lilley [11] (with some aspects again revisited in a later airframe noise study [12]), who discusses Graham's mechanisms for the silent owl flight and concludes that these mechanisms lead to a major noise reduction above 2 kHz. More exactly, he holds the downy upper surface of the feathers (the third mechanism identified by Graham) responsible for the low noise generation of the owls above 2 kHz. Lilley developed a relatively simple noise prediction model for birds and small gliding aircraft. His model is derived from the fundamental theoretical work of Ffowcs Williams and Hall [13] for a flat, semi-infinite plate at zero incidence and consequently only considers trailing edge noise. The resulting model for the prediction of the gliding flight noise only contains two parameters, the mass of the bird or glider (as a measure for its lift in equilibrium flight) and its speed of flight. Other parameters, such as angle of attack or certain boundary layer parameters, are taken to affect the lift force and are hence accounted for. Lilley states that the model is not valid for owls due to the special features of their wings and feathers.

Apart from the examinations of the flight noise produced by owls and birds in general, there exist several aerodynamic studies dealing with bird flight. This includes studies on birds flying in a wind tunnel, like those by Pennycuick [14], Tucker and Parrott [15] and by Brill *et al.* [16]. Those investigations showed that aerodynamic measurements on birds in a wind tunnel are feasible and provide insight in the aerodynamics of birds. Besides measurements on living birds there are a number of aerodynamic wind tunnel studies on prepared bird wings. A basic theoretical work on the aerodynamics of bird wings, including the characterization of the wing data and the flight performance using the terminology of aviation aerodynamics as well as detailed descriptions of the procedure of wind tunnel measurements, was done by Nachtigall [17]. Withers [18] performed an aerodynamic study on eight bird wings and one single feather in a wind tunnel. Like Nachtigall, Withers also used the terminology of technical airfoils for the characterization of the aerodynamic properties of the prepared wings. No silently flying birds were examined in those experiments though. March *et al.* [19] conducted aerodynamic wind tunnel measurements on the prepared wings of a great horned owl (*Bubo virginianus*) as a representative for the silently flying owls and a red-tailed hawk (*Buteo jamaicensis*). Interestingly, they observed a strong twist of the highly elastic wings in the fluid flow and took this into account when discussing the aerodynamic performance. Additionally, they tried to model these aeroelastic effects with computational flow simulation tools. As opposed to the observations made by Kroeger *et al.* regarding the aerodynamic performance of owls, Klän *et al.* [20] examined an owl-based airfoil and argue that the surface structure of the owl wing may contribute to an increase of the aerodynamic performance of the wing by decreasing or suppressing the separation bubble or by stabilizing it. More recently, Winzen *et al.* [21] performed Particle Image Velocimetry (PIV) measurements on a prepared barn owl wing to study flow phenomena like separation, transition, and reattachment, and compared the results to those from Klän *et al.* [20] for the artificial owl-based wing. Interestingly, as opposed to the results obtained for the artificial wing, they did not observe the formation of a separation bubble at all.

These studies show that the acoustics and the aerodynamics of the silent owl flight are still of great interest for use in technical applications, especially against the background of rising requirements to further reduce airframe noise. However, it also becomes apparent that there exist only few publications that allow for a detailed comparison of the noise produced by gliding owls to that of other birds. The main reason is that it is very challenging to give experimental evidence for the lower flight noise generation. Basically, different approaches may be pursued to measure the noise generated by gliding owls compared to that generated by non-silently flying birds. These methods include

- measurements on flying birds and
- measurements on prepared birds or wings.

The first method was successfully realized as microphone array measurements in an outdoor environment on a common kestrel (*Falco tinnunculus*), a Harris hawk (*Parabuteo unicinctus*) and a barn owl by Sarradj *et al.* [22]. Such experiments are very sophisticated since (1) the birds have to be trained to fly along a desired trajectory, (2) measurements of both flight noise and trajectory have to be done without harming the birds or putting stress to the birds, (3) the gliding flight noise levels are very low, which requires a low background noise and a very sensitive measurement equipment and (4) large numbers of flyovers are necessary to achieve a sufficient statistical significance of the results. Additionally, it is very hard to compare the noise of different birds. In the end, the results from Sarradj *et al.* showed that the noise generated by the owl is significantly lower than that generated by the kestrel and the hawk in a frequency range above 1.6 kHz.

The second method, acoustic measurements on prepared wings, has the advantages that the experiments can be performed in an acoustically treated lab environment, as for example an aeroacoustic wind tunnel, and that the flow speed can be varied at will. Initially, this approach seems to be more simple regarding both the setup and the reproducibility of the experiments. For such an experimental study the shape of the prepared wings plays a more important role. Due to the process of preparation it is not possible to obtain wings that have exactly the same properties as the wings of a living bird, and hence the prepared wings to be used have to be chosen carefully and their aerodynamic properties have to be considered at the same time.

The research presented in this paper focuses on the analysis of the silent flight of owls using the second method, experiments in an aeroacoustic wind tunnel. Preliminary results of such measurements on only two specimen are briefly described by the authors [23]. The aim of the present paper is the comparison of the noise generation at the wings of owls to that at wings from birds that do not fly silently. The focus herein is on the gliding flight only, where the wing position is fixed without any flapping motions. The measurements were conducted in an aeroacoustic wind tunnel on prepared bird wings using microphone array measurement technique. Additionally, the aerodynamic performance of the wings is taken into account. Of course, the prepared wings behave differently in a flow than wings of a living bird during flight, as their shape is not adjusted to the according flight situation and the instantaneous flow field. However, wind tunnel measurements, as opposed to experiments on flying birds, have the advantage of more repeatable measurement conditions, independent of the behavior and training of a bird and the possible influence of the weather.

The remainder of this paper is organized as follows: First, the experimental setup is described. This includes the prepared bird wings available for this study, the aeroacoustic wind tunnel, the measurement of the aerodynamic performance of the wings, the microphone array used for the acoustic measurements and the subsequent processing of the acoustic data. Then, the results of the aerodynamic and the acoustic measurements are presented and discussed.

2. Experimental Setup

2.1. Prepared Wings

The prepared wings of five different species were examined in the experiments described in the present paper, using two specimen from each species. The species included the tawny owl (*Strix aluco*) and the barn owl (*Tyto alba*) as representatives of the silently flying birds. In contrast, wings of the common buzzard (*Buteo buteo*), the eurasian sparrowhawk (*Accipiter nisus*) and the pigeon (*Columba livia*) represented the non-silently flying birds. Pigeons, although no birds of prey, are known as fast flyers and are thus included in the study. A photograph of each wing can be seen in Figure 1. The ten specimen were selected carefully out of a total set of 42 wings depending on suitability for the purpose of the experiments. The wings of both owl species, the buzzard wings and the sparrowhawk wings were provided by the *Senckenberg Naturhistorische Sammlungen Dresden*. The wings of the pigeon were provided by the *Institute for Biology II, Department of Zoology and Animal Physiology* of the *RWTH Aachen University*.

2.1.1. Description of the Prepared Wing Specimen

When using prepared wings for aeroacoustic and aerodynamic wind tunnel measurements, it is obvious that such specimen do not exactly represent the wings of living birds in gliding flight in their complex three-dimensional shape in every detail, but rather reduced models that can be used when the deviations from a real wing are considered. In the present case, the basic process of the preparation was the following: The wings were separated from the bodies and the muscle tissue was removed from the bones. The wings were then manually extended until they were sprawled out

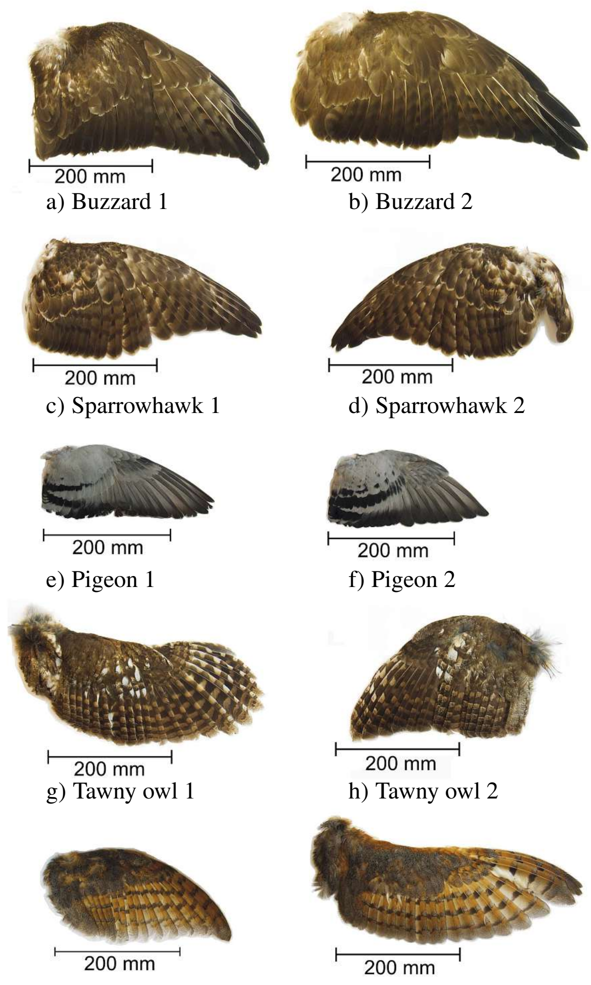

Figure 1. Bird wing specimen used for the present experiments.

and finally they were dried. Some of the wings from Figure 1 are specimen that were not specially prepared for the purpose of this study, but were prepared at an unknown time in the past. It has to be kept in mind that differences in elasticity and tension of muscles and tendons between living and dead birds are generally unavoidable and remain a source of error [24]. As a result, the process of the preparation has an effect on aerodynamic parameters like the spanwise distribution of camber, thickness and twist [5]. Additionally, the flexibility of the wing specimen, as opposed to rigid airfoil models, may affect the aerodynamics. However, if measurements on bird wings in a wind tunnel are desired, then the process of preparation is inevitable and its influence on the experimental results has to be discussed accordingly.

Basically, in order to examine the noise generation of owl wings compared to that of the wings of non-silently flying birds, another possible method would be the use of freshly dead bird wings. Of course, the wings would then have to be supported to obtain the shape of a gliding wing, which is very difficult, but the influence of the preparation on the wing parameters could be neglected. Still, both the use of prepared wings and the use of freshly dead bird wings suffer from the same problem: their complex shape cannot be controlled actively and may be different from that of the wing of a living bird. The only way to ensure that the wing is shaped in a natural form is to perform flyover noise measurements, as done by the authors [22]. In contrast, the present experiments on prepared wings intentionally represent a complementary study to such flyover measurements, which has the previously discussed advantages that the measurements are reproducible and that the flow speed can be varied at will.

The three-dimensional shape of the examined wings, which, as mentioned above, has a noticeable effect on the aerodynamic and the acoustic performance, was fixed in the present study due to the preparation. The wings were not swept during the measurements. Their shape is assumed to correspond approximately to the shape of a wing during the gliding phase of the flight. However, similar to the approach used by Lilley [11] for the development of his flight noise prediction model, the hypothesis of the present work is that the wing shape (and subsequently also the deviation of the shape of a prepared wing from that of a living, gliding bird) as well as possible imperfections of the wings (such as missing feathers) have an influence first and foremost on the aerodynamic performance of the wing, as they would in a living bird. In reverse, the aerodynamic parameters, if known, can then be included in the analysis of the acoustic data to account for differences in wing shape.

As explained above, the selected specimen are the ones that were found to be best suited for the intended experiments despite some minor restrictions. These restrictions will be briefly discussed:

- Certain wings show small imperfections, for example the missing ninth and tenth primary feather of the second pigeon wing, Figure 1f.
- The shape of some wings is somewhat flexed, for example the wings of the buzzard, Figure 1a and Figure 1b. They may have been prepared in relation to the hunting behavior of the buzzard: To catch the prey, the bird maximizes its speed in a dive by bringing its wings closer to the body, still without any flapping of the wings. The shape of the prepared buzzard wings available for this study apparently resembles a condition where the bird starts this diving phase.
- Even the individual wings of one species may have a more or less different shape and wing area, as for example the two wings of the tawny owl, Figure 1g and Figure 1h: While the first wing is fully extended and noticeable tip slots have been formed, the second wing is flexed to a certain degree.

2.1.2. Characterization of Prepared Wings using Airfoil Terminology

The geometry of the wings of the present study is described by the wing area A, the effective wing area A_{eff}, the wing halfspan h_s and the effective wing halfspan $h_{s,\mathrm{eff}}$, which were measured using a *Microscribe G2* three-dimensional digitizer. The effective wing area is the part

Table I. Data of the prepared bird wings (effective wing area A_{eff}, effective halfspan $h_{s,\text{eff}}$, averaged chord length $\overline{c}_l$ and aspect ratio ar).

No	wing		side	A_{eff} [m^2]	$h_{s,\text{eff}}$ [m]	$\overline{c}_l$ [m]	ar	Figure
1	Common buzzard	*Buteo buteo*	right	0.0484	0.381	0.127	0.33	1a
2	Common buzzard	*Buteo buteo*	right	0.0462	0.384	0.120	0.31	1b
3	Eurasian sparrowhawk	*Accipiter nisus*	right	0.0423	0.360	0.117	0.33	1c
4	Eurasian sparrowhawk	*Accipiter nisus*	left	0.0365	0.355	0.103	0.29	1d
5	Pigeon	*Columba livia*	right	0.0186	0.241	0.077	0.32	1e
6	Pigeon	*Columba livia*	right	0.0174	0.228	0.076	0.33	1f
7	Tawny owl	*Strix aluco*	right	0.0466	0.287	0.162	0.56	1g
8	Tawny owl	*Strix aluco*	left	0.0382	0.320	0.120	0.37	1h
9	Barn owl	*Tyto alba*	right	0.0278	0.285	0.098	0.34	1i
10	Barn owl	*Tyto alba*	right	0.0448	0.334	0.134	0.40	1j

of the complete wing area exposed to the flow during the measurements in the wind tunnel, in other words the area that solely contributes to the lift of the wings (in some publications also called the "projected" area). The photographs in Figure 1 correspond to the total wing area A. Subsequently, the effective halfspan is the spanwise length of the wing measured from the point on the leading edge where the wing is exposed to the flow to the wing tip (the tip of the longest primary feather). In accordance to Withers [18], the averaged chord length $\overline{c}_l$ is then defined as the ratio of effective wing area to effective halfspan,

$$\overline{c}_l = \frac{A_{\text{eff}}}{h_{s,\text{eff}}} \tag{1}$$

and the aspect ratio ar is defined as the ratio of effective wing area to the square of the effective halfspan,

$$ar = \frac{A_{\text{eff}}}{h^2_{s,\text{eff}}}. \tag{2}$$

Effective wing area A_{eff}, effective halfspan $h_{s,\text{eff}}$, averaged chord length $\overline{c}_l$ and aspect ratio ar for each wing specimen examined in the present study are given in Table I.

The angle of attack α of the wings in the flow was measured at mid-span, as proposed by Withers [18]. This was done when the wind tunnel fan was off, using an electronic water level held under the wing. Therefore, the measured angle is actually slightly smaller than the exact angle of attack at mid-span which is defined as the angle between the main flow direction and the chord (see Figure 2). Of course the definition of one angle of attack for such a complex-shaped object as a bird wing is a considerable simplification.

It is known that the presence of a flow affects the effective angle of attack and the camber of a bird wing [25]. The angle of attack α is also expected to affect the noise generation in the flow, although mainly at low frequencies around the peak of the noise spectrum. At high frequencies, a change in angle of attack seems to have no noticeable influence on the resulting spectra, as can be seen from results of acoustic measurements on technical airfoils, as for example described by Hutcheson and Brooks [26].

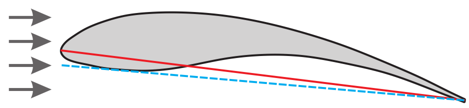

Figure 2. Measurement of the angle of attack at midspan. Dashed: line along which the angle of attack was measured, solid line: exact chord line (Note that the airfoil shown is not a biological one, but a technical airfoil given for the purpose of illustration only.)

Due to these reasons, the simplified procedure of measuring the angle at mid-span is a limitation of this study, since spanwise variations of the angle of attack caused by flow-induced motions of the wing are not taken into account. A more exact method to measure the angle of attack and its spanwise distribution, like a three-dimensional scan of the wing shape, was not available. Additionally, the changes of the angle of attack due to the flow would have to be analyzed for each flow speed and the angle of attack would have to be readjusted accordingly. However, the purpose of this study is the comparison of the noise generation at the wings of silently flying birds to the noise generation at the wings of non-silently flying birds at comparable angles of attack. Therefore, special care has been taken to adjust the angle in a similar way for each prepared wing. If it is assumed that slight deviations of the angle of attack mainly affect the lift generation of the wings, while their influence on the acoustic spectra can be neglected in the frequency range of interest, then the application of scaling approaches that make use of the measured lift forces will remove the influence of such differences.

2.2. Wind Tunnel

The measurements took place in the aeroacoustic wind tunnel at the Brandenburg University of Technology in Cottbus, which is an open jet wind tunnel. The circular nozzle used for the experiments has an exit diameter of 0.35 m, the maximum flow speed with this nozzle is approximately 25 m/s. The turbulence intensity in front of the nozzle and the corresponding velocity profile are given in Figure 3 for two adjusted flow speeds U_0. It can be seen

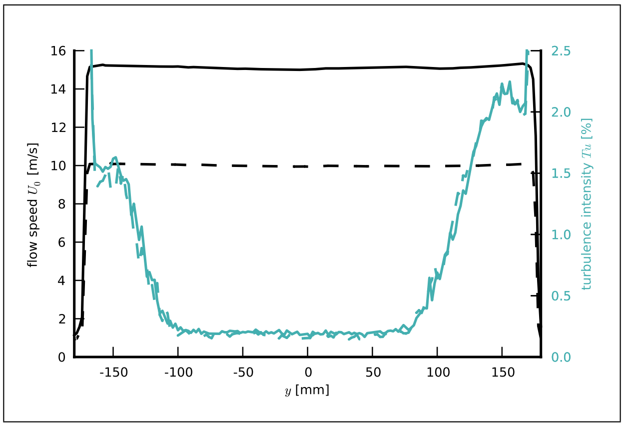

Figure 3. Velocity profile (black lines) and turbulence intensity (grey lines) of the nozzle, measured along a horizontal line, U_0 = 15 m/s (solid lines), U_0 = 10 m/s (dashed lines).

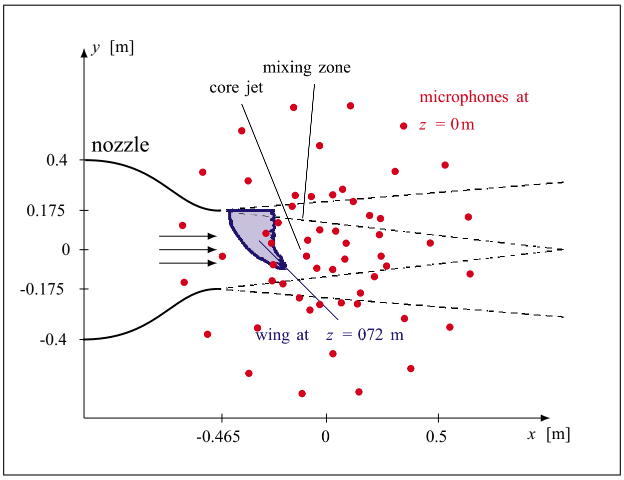

Figure 4. Schematic display of the measurement setup (top view). Note that only the effective "projected" area of the wing is shown.

that the flow inside the core jet has a low turbulence intensity in the order of 0.2 % and less. The overall A-weighted sound pressure level of the wind tunnel background noise at 20 m/s is below 44 dB, measured at a distance of 1 m at 90° to the wind tunnel axis.

During acoustic measurements, the test section is surrounded by a cabin with sound absorbing side walls that provide full absorption for frequencies greater than 500 Hz. The side opposite to the wind tunnel nozzle is open. The cabin has a width of 1.55 m, a height of 1.5 m and a length (in streamwise direction) of 2 m. Figure 4 shows a schematic of the experimental setup. Additional information on the aeroacoustic wind tunnel are given by Sarradj *et al.* [27]

The dimensions of the wings (see Table I) are not negligible compared to the jet width, which leads to the effect of a partial blockage of the wind tunnel, especially at higher angles of attack. This blockage, which has an impact on the aerodynamic loading of the wings positioned in front of the nozzle, as well as the fact that the flow field around the wings changes in the spanwise and the chordwise direction due to the expanding jet width, are effects that usually require a correction of the angle of attack. Such a correction yields an effective angle of attack to account for differences between the flow field in the open jet compared to free flow conditions. Unfortunately, common correction procedures, like those proposed by Brooks *et al.* [28, 29], are more or less inapplicable to this study. The main reason is that the prepared wings are no ideal technical symmetrical airfoils, but cambered biological airfoils with complex shapes. Furthermore, the blockage of the nozzle changes due to the elasticity of the wings, while additionally each of the prepared bird wings is, at least to a certain degree, permeable to the air flow, which further reduces the effect of blockage compared to common technical airfoils. In general, at low angles of attack the influence of the blockage is very small only.

2.3. Aerodynamic Performance

A six-component balance was used to measure the lift force F_L that acts on the prepared wings as a measure of their aerodynamic performance. The balance consists of six single point load cells. The data were measured with a sample rate of 1 kHz, using a National Instruments 24 Bit full-bridge analog input module, and time averaged.

Since the position of the wings is fixed, the lift force is defined as the vertical force in the positive z-direction, perpendicular to the flow direction. The lift coefficient C_L is then defined by

$$C_L = \frac{2 \cdot F_L}{\rho \cdot U_0^2 \cdot A_{eff}}. \quad (3)$$

Herein, F_L is the measured lift force, U_0 is the flow speed and ρ is the fluid density.

The wings were attached to the balance with a mounting that allows for the adjustment of the angle of attack. The mounting was carefully designed and constructed to meet three requirements: First, no noise should be generated at the mounting, second, no aerodynamic effects should be caused by the mounting and third, the mounting had to tightly grip the wings without destroying the fragile bone- and feather-structure. Additionally, the prepared wing is bedded between two slices of soft polyurethane foam. Figure 5 shows a photograph of the setup, and especially the mounting, which is connected to a three-dimensionally adjustable pan/tilt head. The mounting was positioned out of the flow and the wings were hold in front of the nozzle at the height of its horizontal center plane.

2.4. Microphone Array and Data Processing

2.4.1. Beamforming Algorithms

The noise generated at the prepared wings propagated through the shear layers of the open jet and was measured with the microphone array positioned above the wings outside of the flow. In this study, no shear layer correction, like that published by Amiet [30] and Schlinker and Amiet [31], was implemented. This is due to the fact that the exact geometry of the shear layer is not known and due to the

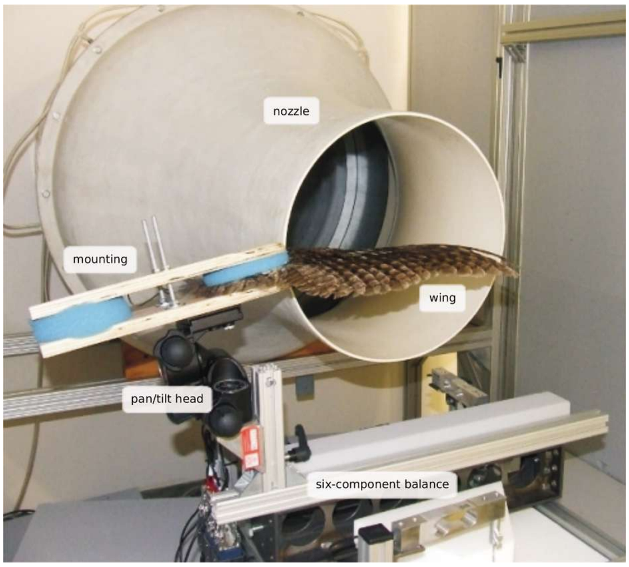

Figure 5. Photograph of the setup including the mounting specially designed to hold the fragile wings and to allow for the exact positioning of the wing in front of the nozzle.

relatively small flow speeds, resulting in only a minor effect of the refraction on the sound source localization and magnitude.

The planar microphone array that was used for the acoustic measurements consists of 56 microphones, the position of which can be seen in Figure 4. It was placed 0.72 m above the prepared wings. Using a 24 Bit National Instruments multichannel measurement system, the acoustic data were recorded with a sample frequency of 51.2 kHz and a total of 2,048,000 samples per channel, corresponding to a measurement duration of 40 s for each acoustic measurement. The sampled time data were Fast Fourier transformed with a Hanning window and 4,096 samples per block and 50 % overlap, resulting in a frequency line spacing of 12.5 Hz. For each block, the cross spectral matrix was calculated and the resulting 999 matrices were averaged.

In a first step, a conventional delay-and-sum beamforming technique [32] was applied to the data, where the signals from each microphone are delayed appropriately, weighted and summed up to obtain maps of the local sound pressure contributions. Such maps show a spatial image of the distribution of noise sources within the source region and can be imagined as an "acoustic photograph". Usually, these maps are two-dimensional representations of the sound pressure contributions located at the grid points of a two-dimensional mapping plane. In the present case, due to the fact that the prepared wings are not in one plane, the beamforming was applied to a fully three-dimensional source volume. Potential noise sources may be located at each grid point of a three-dimensional grid. Therefore, the three-dimensional beamforming provides a better depth resolution than conventional two-dimensional beamforming. The resulting "sound maps" are three-dimensional images of the sound sources. This method was, for example, successfully applied to the measurement of the flow-induced noise from high-speed trains by Brick *et al.* [33] and to airfoil leading edge noise measurements by Geyer *et al.* [34]

When three-dimensional beamforming is to be applied, a source grid with a noticeably increased number of grid points is necessary to obtain a sufficient resolution. In the present case, the grid had an extent of 0.5 m in the streamwise (x-) direction, 0.6 m in the lateral (y-) direction and 0.6 m in the vertical (z-) direction. With an increment of 0.01 m this lead to a total number of 189,771 grid points.

To further process the data and to remove the influence of side lobes, different deconvolution algorithms were initially considered, including

1. the DAMAS (Deconvolution Approach for the Mapping of Acoustic Sources) beamforming algorithm [35], an algorithm that computes a theoretical point spread function between the points in the map and iteratively calculates the source strengths (thus removing the influence of side lobes),
2. the CLEAN-SC beamforming algorithm [36] that uses the spatial coherence between points in the sound map instead of a theoretical point spread function and
3. the orthogonal beamforming (OB) algorithm [37] that performs an eigen-decomposition of the cross-spectral matrix to obtain a number of point sources smaller than or equal to the number of microphones.

The DAMAS algorithm iteratively solves a system of equations that contains as many equations as there are points in the grid by using a special Gauss-Seidel-technique. It is known to deliver reliable results in aeroacoustic testing, also at low frequencies. Unfortunately, due to the increased number of grid points necessary for three-dimensional beamforming, the DAMAS is computationally too expensive and hence, at this point in time, not feasible for the processing of the present data. The CLEAN-SC algorithm performs faster than the DAMAS. It is known to give good results at low and medium frequencies but, in some cases, was found to miss high frequency noise sources that are relatively weak [38]. This may be important for the present investigation because the noise sources located on the surface of wings of silently flying owls are expected to be relatively weak. The orthogonal beamforming method also performs faster than the DAMAS and tends to give reliable results over a large range of frequencies. At low frequencies, the noise source localization may be imprecise.

It was finally decided to use the CLEAN-SC algorithm for the processing of the acoustic data due to its overall good performance in the frequency range of interest. The main diagonal of the cross-spectral matrix was removed to eliminate the influence of channel self noise on the beamforming result.

Figure 6 shows a projection of three-dimensional sample sound maps, obtained for measurements at two specimen, a buzzard wing and a tawny owl wing. It is visible that the noise generated at the prepared wing of the buzzard exceeds the noise generated by the owl wing by about 10 dB in the 4 kHz octave band and about 18 dB in the

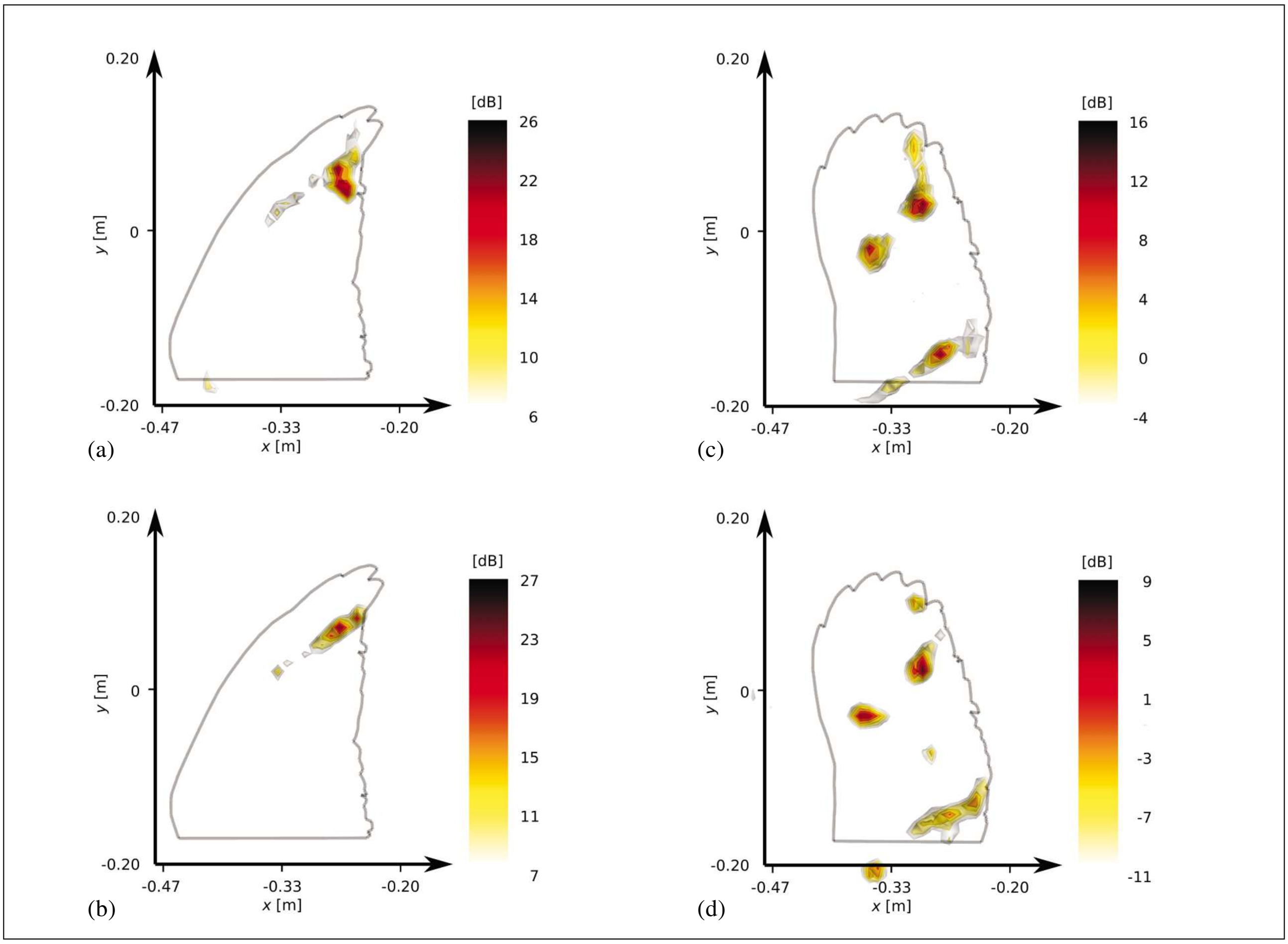

Figure 6. Projection of three-dimensional CLEAN-SC sound maps, top view, flow speed $U_0 \approx 12$ m/s. a) Buzzard wing (Figure 1a), 4 kHz octave band, b) Buzzard wing (Figure 1a), 8 kHz octave band, c) Tawny owl wing (Figure 1g), 4 kHz octave band, d) Tawny owl wing (Figure 1g), 8 kHz octave band.

8 kHz octave band. The sound maps also show that the noise sources are positioned near the wing tip in case of the buzzard, while they are positioned on the wing surface in case of the owl. This is in accordance to the results from flyover measurements [22].

For technical wings in a virtually non-turbulent flow, it would be expected that the noise sources are located at the trailing edge or the wing tip. A possible reason for the location of the sources on the surface of the tawny owl wing rather than near the trailing edge or the wing tip is that the special feather adaptations of the owl indeed lead to a noticeable reduction of these major noise sources. Hence, the sources that are now visible are only the remaining, much weaker sources.

Additional weaker sources can also be found at the side of the wing near the position where the wings are mounted to the six-component balance. It can be assumed that these sources are caused by the turbulent shear layer interacting with the wing. The amplitude of these weaker noise sources is noticeably smaller than that of the main sources.

2.4.2. Sound Pressure Level Spectra

To obtain absolute sound pressure levels of the noise generated by the wing specimen, the resulting CLEAN-SC sound maps were integrated over a volume that contains the main wing area in front of the wind tunnel nozzle, but neither the nozzle itself nor the shear layers. At the position of the trailing edge of the first buzzard wing, which is the specimen with the largest streamwise extent, the shear layers have a distance of approximately 0.3 m. Thus the defined volume has a spanwise extent of only 0.28 m, to exclude the impingement of the shear layers on the wings, a vertical extent of 0.20 m and a streamwise extent of 0.30 m. It can be seen in Figure 7. Noise sources such as the weaker sources seen in Figures 6c and 6d, which are generated due to the interaction of the shear layer with the wing surface, are thus excluded from the integration.

The result of the integration is the contribution of the sound pressure that is generated within the chosen volume, measured in the array center. These results were then transferred to third octave band sound pressure levels (L_p), relative to $p_0 = 2 \cdot 10^{-5}$ Pa, with center frequencies between 630 Hz and 16 kHz. The lower frequency limit was chosen with respect to the limit of the measurement setup. For frequencies below the 630 Hz third octave band, the measured sound pressure level spectra suffered from the contamination with noise originating from standing waves in the measurement setup. The upper frequency limit was

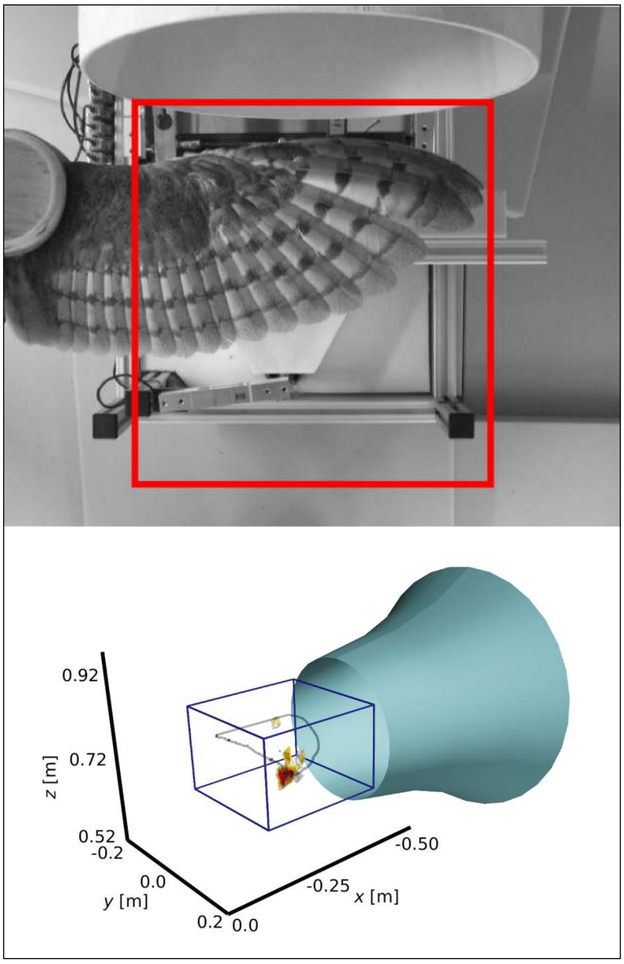

Figure 7. Schematic of the volume used for the integration (0.30 m x 0.28 m x 0.28 m). Above: Top view, below: schematic (three-dimensional sound map shows 4 kHz octave band of the first buzzard wing, corresponding to Figure 6a).

chosen due to the possible contribution of high frequency noise which is reflected at certain parts of the measurement setup.

3. Results and Discussion

Acoustic and aerodynamic measurements were conducted on the ten wings specified in Table I at three different angles of attack (0°, 8° and 16°) and 15 flow speeds between 5 m/s and 20 m/s. For the first buzzard wing, measurements were performed at flow speeds above 12 m/s only, for some other wings additional measurements were performed at different angles of attack. This led to a total amount of raw acoustic data of more than 200 GByte. However, the present paper focuses on the results obtained at zero angle of attack since, as discussed in the previous section, non-zero angles lead to a more complex flow field around the wing and, in some cases, to a change of the wing shape. Additionally, the effect of blockage, as discussed in section 2.2, is negligible at zero angle of attack.

As already mentioned above, owls do not fly very fast, especially in gliding flight. According to Neuhaus *et al.* [9] the maximum speed of the tawny owl is only about 6 to 10 m/s. According to Mebs and Scherziger [39], owls tend to fly even slower, with speeds in the range of 2.5 m/s to 7 m/s. The higher speeds are mainly given here to provide sufficient data for the non-silently flying birds of prey, since they fly, on average, with a speed of 10 m/s and more (the mean flight speed of the pigeon even exceeds 15 m/s) [40].

3.1. Aerodynamic Results

Prior to the presentation of the acoustic results, the results of the aerodynamic measurements on the wing specimen from Table I are presented since they will be used to scale the measured acoustic data.

Figure 8 shows the measured lift coefficient, calculated using Equation (3), as a function of the flow speed U_0 for zero angle of attack. It was decided to show the results for both specimen of each species rather than giving an average. This is due to the fact that, as mentioned before, the preparation does affect the aerodynamics and acoustics of each wing and cannot be neglected, and hence an average over the results obtained for two representatives of each species would only give the wrong impression of a generalization of the measured data. The aerodynamic data obtained for the two pigeon wings are only available for the higher flow speeds.

At zero angle of attack the lift curves of the prepared wings remain nearly constant over the whole range of flow speeds. This is in accordance with the aerodynamics that would be expected for technical wings and airfoils. The owl wings clearly produce the highest lift coefficient. It is approximately twice as high as the lift coefficient of the buzzard wings, which generate the smallest lift coefficient. The facts that the lift coefficient of both buzzard wings is comparatively small and that the second tawny owl wing generates less lift than the first specimen may also be influenced by the somewhat flexed shape of these wings. The mean values of the lift coefficients C_{L}, averaged over the values for each flow speed, as well as the corresponding standard deviations are given in Table II for each wing specimen.

Included in Figure 8 are the data obtained by Withers [18] for the wing of a red-shouldered hawk (*Buteo lineatus*) and the data measured by March *et al.* [19] for the left wing of a great horned owl (*Bubo virginianus*). The hawk wing, which was chosen from the different wings examined by Withers as a means of comparison for the aerodynamic results presented here, had a length of 0.394 m and a projected area of 0.052 m^2. It is therefore somewhat larger than the buzzard wings of the present study. The results obtained by Withers for the lift coefficient at zero angle of attack, given in [18] as mean value and deviation, are in close agreement with the values obtained for the buzzard wings. Furthermore, it is stated in [18] that the lift coefficient is independent of velocity in the examined range of flow speeds, which is also confirmed by the present findings. Withers performed his measurements in a Reynolds number range from $1{\cdot}10^4$ to $4{\cdot}10^4$, approximately corresponding to speeds below 6 m/s.

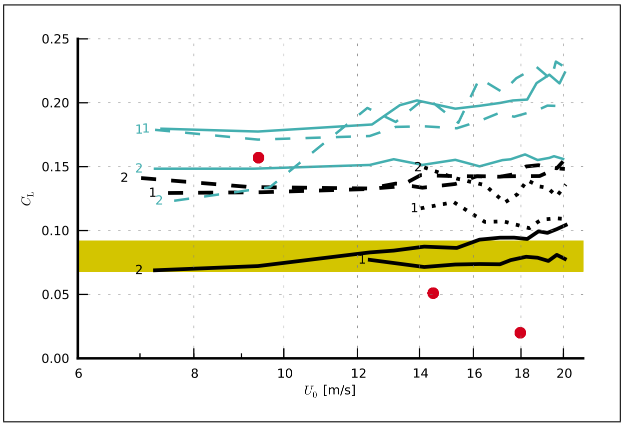

Figure 8. Comparison of the lift coefficient, angle of attack α = 0° (black solid line: buzzard, black dashed line: sparrowhawk, grey solid line: tawny owl, grey dashed line: barn owl), numbers indicate first and second specimen from each species, grey underlayed: red-shouldered hawk with data from Withers [18], •: great horned owl with data from March *et al.* [19]).

Table II. Mean lift coefficients $\overline{C_L}$, averaged over the values for each flow speed, and corresponding standard deviation σ_{C_L} of the prepared bird wings.

No	wing	$\overline{C_L}$	σ_{C_L}
1	Buzzard 1	0.076	0.003
2	Buzzard 2	0.090	0.010
3	Sparrowhawk 1	0.142	0.008
4	Sparrowhawk 2	0.141	0.005
5	Pigeon 1	0.109	0.006
6	Pigeon 2	0.135	0.007
7	Tawny owl 1	0.201	0.014
8	Tawny owl 2	0.154	0.003
9	Barn owl 1	0.186	0.009
10	Barn owl 2	0.198	0.033

The data on the great horned owl wing, that had a half span of 0.648 m and an area of 0.126 m^2, were obtained from diagrams in [19] that present the lift and drag coefficients as a function of angle of attack for four different flow speeds. The lift coefficient of the great horned owl's wing is comparable to the results of the bird wings used in the present study at a low flow speed of 9.39 m/s. Curiously, the values of the lift coefficient measured by March *et al.* strongly decrease with increasing flow speed, an effect that may have been caused by the mounting of the wing (March *et al.* inserted a thin aluminum rod into the leading edge along the wing which was fixed to a six-degree-of-freedom strain gorge force balance). At low flow speeds, March *et al.* state that the lift coefficient is higher since the wing is less deformed, while the deformation is significant at high speeds and high angles of attack. No such strong deformation was observed in the present study. In their PIV measurements on a prepared barn owl wing, Winzen *et al.* [21] also observed a "straightening of the wing" with increasing flow speed. However, the maximum local displacement of the wing surface they measured was relatively small (in the order of 1 mm at zero angle of attack and still below 4 mm at an angle of attack of 6°) for flow speeds from 3.5 m/s to 10.5 m/s, but no strong deformation occured.

It can be concluded from the results shown in Figure 8 and Table II that, on average, the owl wings examined generate a relatively high lift coefficient that exceeds the lift coefficient of the wings from the non-silently flying birds. This result supports the statement [20, 21] that the properties of the owl wings increase aerodynamic performance by increasing lift (and decreasing drag), which is necessary to fly effectively at low flow speeds.

3.2. Acoustic Results

In this section, the results from the acoustic measurements are presented. The noise generation of the prepared bird wings in the wind tunnel is a function of both frequency f and flow speed U_0. Figure 9 shows this dependence for zero angle of attack in the form of contour plots for the power spectral density in third octave bands with the center frequency f_c for all ten specimen from Table I.

As one would expect, the figures illustrate that in general the noise generated at the prepared wings increases with increasing flow speed and with decreasing frequency. Regarding the maximum amplitude, it can be seen that the highest levels were measured for the second buzzard wing (30 dB) and the first sparrowhawk wing (34 dB), whereas the lowest maximum power spectral density levels were measured for both pigeon wings (21 dB and 22 dB). Thereby, it has to be kept in mind that the wings of the pigeon are also by far the smallest wings examined (see Table I), and hence it is quite reasonable that they do not produce a very high total noise level. This circumstance will have to be considered in a following scaling approach. The second tawny owl wing also generated a relatively low maximum power spectral density level of 23 dB.

In order to account for differences in size and shape of the wings, the aerodynamic performance of the wings is included in the acoustic analysis. Such approaches are often used for the scaling of airframe noise, where, besides flow speed, use is made of aircraft parameters like weight and wing area (see for example the report by Lasagna *et al.* [41]). In the present paper, following the model of Lilley [11], the sound pressure levels are scaled by using the measured lift force F_L according to

$$L_{p,\text{scaled}} = L_p - 10 \cdot \log_{10} \frac{F_L}{F_{L,0}} \text{ dB}, \quad (4)$$

where $F_{L,0}$ = 1 N. This approach was derived based on the fact that in equilibrium flight the weight of the bird is equal to the lift force, and the resulting sound pressure levels can be understood as the noise generated per unit lift force. As stated in section 2.1, a scaling that uses the measured lift forces can be expected to remove the influence of potentially remaining deviations of the adjusted angle of attack.

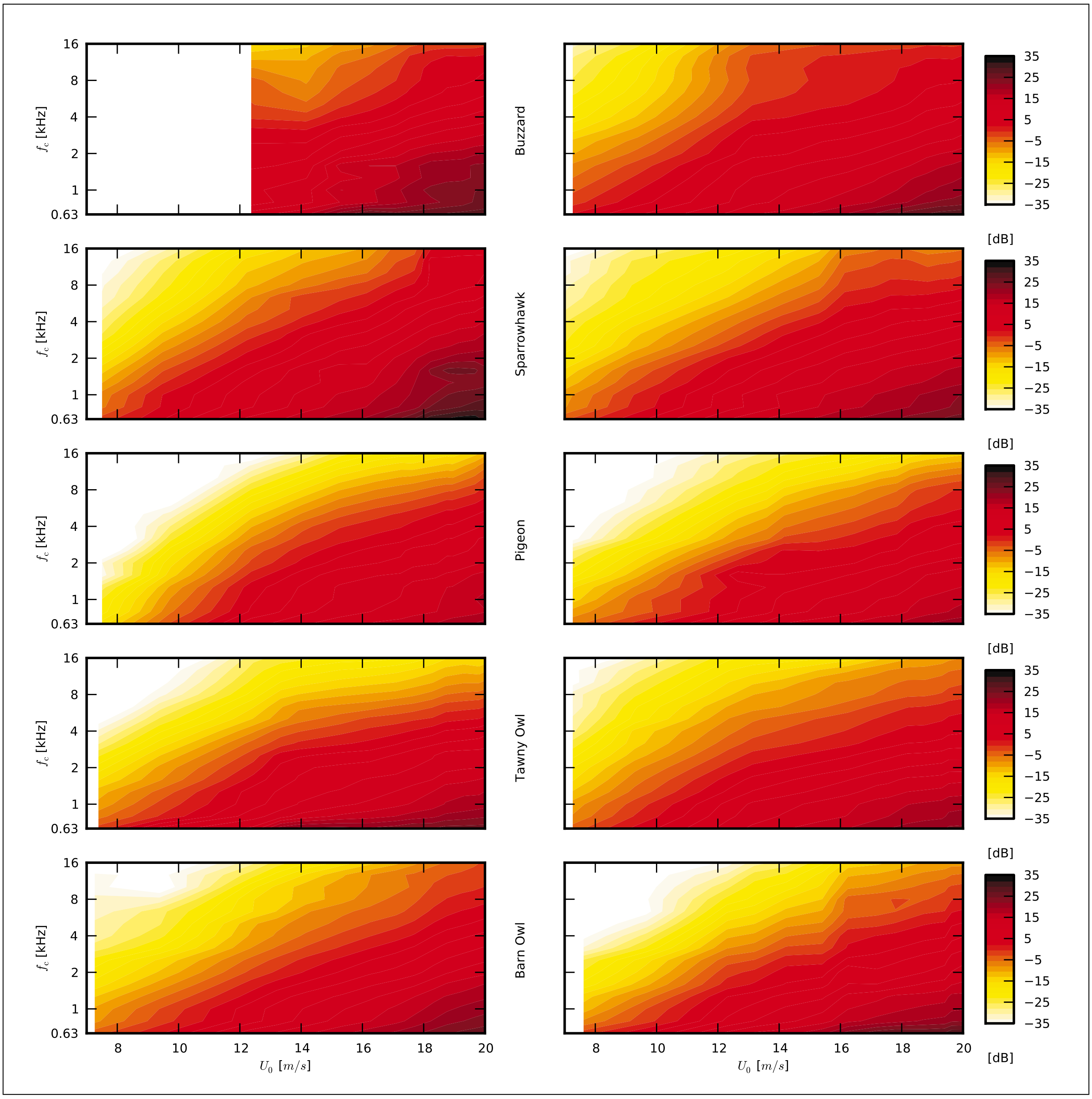

Figure 9. Power spectral density (re $4 \cdot 10^{-10}$ Pa^2/Hz) as a function of third octave band center frequency and flow speed, angle of attack $\alpha = 0°$, as measured in the sector presented in Figure 7 (left column: first specimen, right column: second specimen). Note that measurements of the noise generated by the first buzzard wing were performed at flow speeds above 12 m/s only.

The initial hypothesis of the research was that wings from birds that feature the special plumage adaptations identified by Graham [2] emit less noise in gliding flight than wings from birds without these adaptations. To test this hypothesis using the scaled sound pressure level, values for different birds were compared. These levels depend on both frequency and flow speed. Without using further assumptions on these dependencies, values for different species can only be compared for the same frequency band and flow speed.

The five different species in the present study lead to ten inter-species comparison possibilities (tawny owl – buzzard, tawny owl – sparrowhawk, tawny owl – pigeon, tawny owl – barn owl, barn owl – buzzard, barn owl – sparrowhawk, . . .). For each of these, between 570 and 780 pairs of values for the same frequency band and flow speed could be drawn from the measured results. As the values could not be assumed to be normally distributed, Wilcoxon signed-rank tests [42] were performed for the null hypothesis that the median for the values for species A is equal to or greater than that for species B (one-sided test). On a significance level of 0.1 %, the results of these tests showed that this null hypothesis had to be rejected in favour of the alternative hypothesis that the values for species A are smaller than that for species B ($N = 570 \ldots 780$, $p = 0.0$) with the only exception of the comparison between the two owl species, where the null hypothesis could not be rejected ($N = 750$, $p = 0.00124$). From these results, a ranking for the five species regarding the noise per unit lift force could be established, where the buzzard wings generate the most noise, followed by the sparrowhawk wings, the pigeon wings, and finally the barn owl wings and the wings from the tawny owl. Thus, it could be concluded that for the wings of both owl species the noise was less than for any other species considered in the present study.

In order to allow for a further comparison of the noise generated by the wings from different species, including all measured frequencies and flow speeds, the third octave band sound pressure level spectra are plotted versus a Strouhal number $Sr = f_c \cdot x_0/U_0$. For technical airfoils, it is common to use a dimension of the boundary layer, such as the boundary layer thickness or the boundary layer displacement thickness as dimension x_0. However, no boundary layer parameters were available for the prepared wings. Instead, x_0 is taken as an arbitrary dimension, which was chosen to equal 1 m. Additionally, besides the scaling with the measured lift forces, the third octave band spectra are scaled with the Mach number $Ma = U_0/c$, with c being the speed of sound:

$$L_{p,\text{scaled},2} = L_p - 10 \cdot \log_{10} Ma^3 \text{ dB} - 10 \cdot \log_{10} \frac{F_\text{L}}{F_{\text{L},0}} \text{ dB}. \tag{5}$$

Note that according to basic aerodynamic theory, the lift force is proportional to the square of the flow speed, $F_\text{L} \propto U_0^2$, and hence the approach given by Equation (5) effectively represents a scaling with the fifth power of the flow speed. A scaling with Ma^5 or U_0^5 is commonly used for the presentation of edge noise [13], taking into account that such noise sources are essentially dipole (or "baffled" dipole [43]) in nature. This approach was also applied to the results of the flyover measurements made by the authors [22].

Figure 10 shows the resulting scaled third octave band sound pressure levels generated by the wings as a function of Strouhal number. It is visible that, overall, the implicit scaling with the fifth power of the Mach number according to Equation (5) leads to satisfying results. It can therefore be concluded that, although the noise sources may be located anywhere on the surface of the prepared wings, the directivity is close to that of a baffled dipole or a dipole. However, the fact that the results displayed in Figure 10 still show some scattering implicates that a scaling with U_0^5 does not have to be generally valid for all species examined. It is also possible that slightly different scaling exponents for different species lead to a better collapse of the data. This would be in agreement with the work of Lilley [11], who, while stating that the noise from non-silently flying birds scales with U_0^5, proposes that the noise generated by owls is rather proportional to U_0^6. A detailed investigation of this effect was done by Jaworski and Peake [44] on the more general subject of poroelastic airfoils.

It can be seen from Figure 10 that on average the examined owl wings generate a lower noise level per unit lift force than the wings of the non-silently flying birds of prey (buzzard and sparrowhawk). Due to the fact that the lift coefficient of the pigeon wings is very low (see Figure 8), it is visible that the noise per unit lift force generated by the owl wings is also lower than that generated by the pigeon wings. In general, the differences between the sound pressure level generated by the owl wings and that generated by the non-silently flying birds' wings increase with increasing Strouhal number, which is in accordance to the findings from flyover measurements [22]. The difference between the noise generated by the buzzard wings and the sparrowhawk wings and that generated by the owl wings is noticeable, especially at high Strouhal numbers.

Due to the limited frequency range of the acoustic measurements, it is not possible to draw conclusions on the noise generation at lower frequencies. A comparison between the examined bird wings and technical airfoils may allow for some further understanding: The spectral shape of noise generated by technical airfoils is characterized by a peak whose frequency and magnitude depend on the dimensions of the airfoil, such as the chord length, and the flow speed (see for example the work of Brooks *et al.* [45]), and a decay towards lower and higher frequencies. No distinct peak is visible in the spectra shown in Figure 10, but only a noticeable decay with increasing Strouhal number. Hence the spectra given in Figure 10 imply that the peak would be found at a frequency below the 630 Hz third octave band. This would be in accordance to the findings from Neuhaus *et al.* [9], who state that the spectral peak in the gliding flight noise of the tawny owl lies between 200 Hz and 700 Hz. However, recent flyover noise measurements [22] showed that the flight noise of owls is significantly below that of non-silently flying birds in a frequency range above 1.6 kHz, and thus at frequencies that are measurable in the present experiments. This observation is also in general agreement with the conclusion drawn by Lilley [11], that the feather adaptations of the owl lead to a flight noise reduction in the frequency range above 2 kHz.

In a next step, the scattered data from Figure 10 are smoothed by applying a LOWESS algorithm [46] on the acoustic data belonging to one species. This is done in order to further emphasize the differences between the noise generated at the wings of the silently flying birds to that of the non-silently flying birds. The resulting smoothed sound pressure level curves, still scaled according to Equation (5) using the flow speed and the measured lift forces, are presented in Figure 11. Now it can be seen more clearly that, on average, the noise generated by the owl wings per unit lift force is less than that of the non-silently flying bird wings. Interestingly, at very high Strouhal numbers the noise generated by the pigeon wings per unit lift force is approximately as low as that generated by the owl wings.

Since the presentation of the results in Figures 10 and 11 as a function of Strouhal number includes the dependence on the flow speed U_0, the results confirm that the silent flight of the owl is indeed a result of its special plumage adaptations and not just a result of its lower speed of flight.

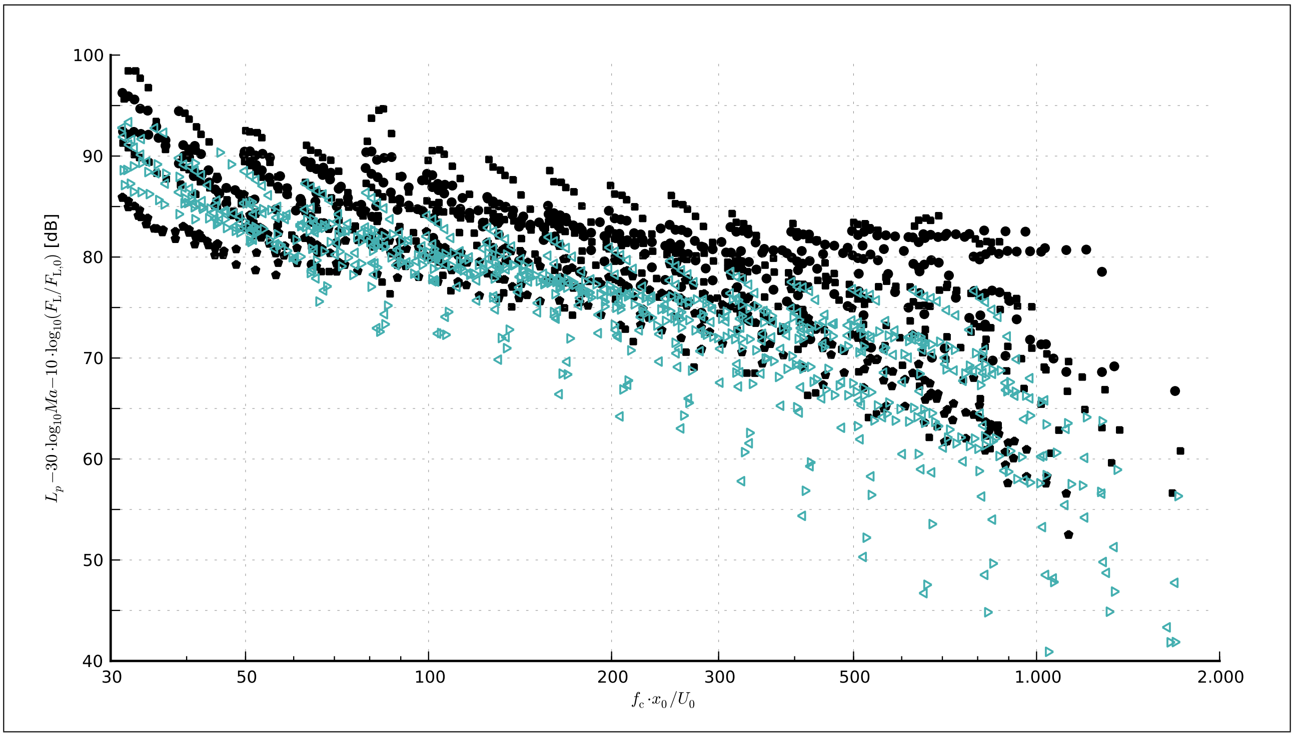

Figure 10. Comparison of the third octave band sound pressure levels, scaled according to Equation (5) using the measured lift forces F_L, as a function of Strouhal number (based on an arbitrary dimension $x_0 = 1$ m), angle of attack $\alpha = 0°$ (•: buzzard, □: sparrowhawk, pentagon: pigeon, ▹: tawny owl, ◃: barn owl).

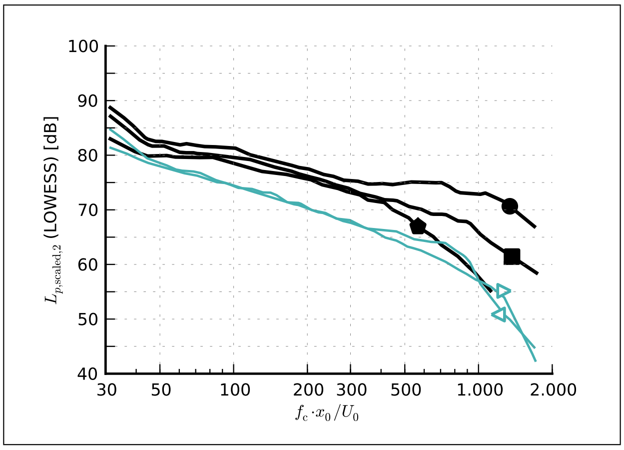

Figure 11. Third-octave band sound pressure levels, scaled according to Equation (5) and smoothed using a LOWESS algorithm [46], angle of attack $\alpha = 0°$ (•: buzzard, □: sparrowhawk, pentagon: pigeon, ▹: tawny owl, ◃: barn owl).

The lower flight speed of the owl under natural conditions compared to the fast flight of the non-silently flying birds of prey only adds to the difference of the gliding flight noise emission. However, the results also reveal that the difference between the sound pressure level generated by the owls and that generated by the non-silently flying birds is not extremely large at all Strouhal numbers, but is still significant. This, too, is in agreement with the results from recent flyover noise measurements [22].

As discussed in section 2.1, there are inevitable deviations of the complex shape and the flexibility of a prepared wing from that of a living bird in gliding flight. Despite this fact, the present results are, to the authors knowledge, the first quantitative acoustic data on the noise generated by wings of owls compared to the wings of non-silently flying birds of prey in a wind tunnel. In order to investigate the particular role of the single plumage adaptations of owls for the silent flight, further research, such as Computational Fluid Dynamics (CFD) studies or the visualization of the flow around an owl wing compared to that around the wing of a non-silently flying bird of prey, may prove helpful. The latter was already done qualitatively by Kroeger *et al.* [7] and by Neuhaus *et al.* [9], who concluded that the leading edge comb merely serves to delay the separation of the flow at near-stall conditions. The PIV study on a prepared wing of a barn owl by Winzen *et al.* [21] was focused on the bending and twisting of the wing due to its elasticity, but the role of the plumage adaptations was not investigated. Therefore, the application of more advanced non-intrusive measurement techniques, like PIV or Laser Doppler Anemometry (LDA), may enable a better quantification of the aerodynamic and acoustic effects of the plumage adaptations.

4. Conclusions

The silently flying species of owls have developed an adapted hunting system that combines a very good hearing to aurally locate the prey with distinct mechanisms of the wings and feathers that enable the nearly silent flight in order to not be heard by the prey.

This paper presents acoustic and aerodynamic results from open jet wind tunnel experiments on prepared wings of five different species, including two silently flying owls. In order to examine the gliding flight noise of birds, these experiments are a complementary approach to flyover noise measurements, although the differences between the shape of a prepared wing and that of a wing from a living, gliding bird have to be kept in mind. The acoustic data were measured using a 56 channel microphone array and analyzed using a deconvolution beamforming algorithm applied to a three-dimensional source region. Sound pressure level spectra were then obtained through integration of the sound pressure contributions over a three-dimensional volume in the sound maps that only contains noise sources at the wing, but not the wind tunnel nozzle or the region where the wind tunnel shear layers interact with the wings. In order to account for the influence of differences in aerodynamic performance on the noise generation that may result from differences in the three-dimensional wing shape, the sound pressure level spectra were scaled with the measured lift forces.

The observation of three-dimensional sound maps reveals that the locations of the noise sources are not necessarily the trailing edge or the wing tips. Although the study is limited concerning the shape and flexibility of the prepared wings available, the resulting sound pressure level spectra clearly confirm that the noise generated by the owl wings in gliding flight is significantly less than that generated by the wings of the non-silently flying birds of prey at the same flow speed. Thus, the experimental results presented in this paper confirm that the silent flight of the owls is indeed a consequence of their special wing and feather adaptations and not only of their lower speed of flight, which is in accordance to the results from a recent flyover noise study.

Acknowledgements

The research presented in this paper was sponsored by the *Deutsche Forschungsgemeinschaft* in the priority program 1207, "Nature Inspired Fluid Mechanics", under the grant number SA 1502/1-2.

The authors are indebted to Dr. Martin Päckert of the *Senckenberg Naturhistorische Sammlungen Dresden* for the helpful discussions and the provision of the wings of buzzard, sparrowhawk, tawny owl and barn owl and to Jens Ziegler for the preparation of those wings. The authors are furthermore indebted to Prof. Dr. Hermann Wagner and Dr. Thomas Bachmann of the *Institute for Biology 2, RWTH Aachen University* for the provision of the pigeon wings and the helpful advise regarding wing shape and condition.

References

[1] E. Mascha: Über die Schwungfedern. Zeitschrift für wissenschaftliche Zoologie **77** (1904) 606–651.

[2] R. R. Graham: The silent flight of owls. Journal of the Royal Aeronautical Society **286** (1934) 837–843.

[3] H. Sick: Morphologisch-funktionelle Untersuchungen über die Feinstruktur der Vogelfeder. Journal für Ornithologie (1937) 206–372.

[4] H. Hertel: Struktur, Form, Bewegung. Otto Krauskopf-Verlag, Mainz, 1963. [translated version: Milton S. Katz (ed.), Structure, Form, Movement. Reinhold, New York (1966)].

[5] T. Bachmann: Anatomical, morphometrical and biomechanical studies of barn owls' and pigeons' wings. PhD-Thesis, RWTH Aachen University, 2011.

[6] W. H. Thorpe, D. R. Griffin: The lack of ultrasonic components in the flight noise of owls compared with other birds. IBIS **104** (1962) 256–257.

[7] R. A. Kroeger, H. D. Gruschka, T. C. Helvey: Low speed aerodynamics for ultra-quiet flight. AFFDL TR 971-75, 1971.

[8] H. D. Gruschka, I. U. Borchers, J. G. Coble: Aerodynamic noise produced by a gliding owl. Nature **233** (1971) 409–411.

[9] W. Neuhaus, H. Bretting, B. Schweizer: Morphologische und funktionelle Untersuchungen über den 'lautlosen' Flug der Eulen (Strix aluco) im Vergleich zum Flug der Enten (Anas platyrhynchos). Biologisches Zentralblatt **92** (1973) 495–512.

[10] G. W. Anderson: An experimental investigation of a high lift device on the owl wing. Master's Thesis, Air Force Institute of Technology, Air University, Wright-Patterson AFB, Ohio, 1973.

[11] G. M. Lilley: A study of the silent flight of the owl. 4th AIAA/CEAS Aeroacoustics Conference, Toulouse, France, 1998, AIAA paper 1998-2340.

[12] G. M. Lilley: The prediction of airframe noise and comparison with experiment. Journal of Sound and Vibration **239** (2001) 849–859.

[13] J. E. Ffowcs Williams, L. H. Hall: Aerodynamic sound generation by turbulent flow in the vicinity of a scattering half plane. Journal of Fluid Mechanics **40** (1970) 657–670.

[14] C. J. Pennycuick: A wind-tunnel study of gliding flight in the pigeon Columba Livia. Journal of Experimental Biology **49** (1968) 509–526.

[15] V. Tucker, G. Parrott: Aerodynamics of gliding flight in a falcon and other birds. Journal of Experimental Biology **52** (1970) 345–367.

[16] C. Brill, D. Mayer-Kunz, W. Nachtigall: Wing profile data of a free-gliding bird. Naturwissenschaften **76** (1989) 39–40.

[17] W. Nachtigall: Vogelflügel und Gleitflug – Einführung in die aerodynamische Betrachtungsweise des Flügels. Journal für Ornithologie **116** (1975) 1–38.

[18] P. Withers: An aerodynamic analysis of bird wings as fixed airfoils. Journal of Experimental Biology **90** (1981) 143–162.

[19] A. March, C. Bradley, E. Garcia: Aerodynamic properties of avian flight as a function of wing shape. ASME International ME Congress and Exposition, Orlando, FL, 2005.

[20] S. Klän, S. Burgmann, T. Bachmann, M. Klaas, H. Wagner, W. Schröder: Surface structure and dimensional effects on the aerodynamics of an owl-based wing model. European Journal of Mechanics B/Fluids **33** (2012) 58–73.

[21] A. Winzen, S. Klän, M. Klaas, W. Schröder: Flow field analysis and contour detection of a natural owl wing using PIV measurements. – In: Nature-Inspired Fluid Mechanics **119**. C. Tropea, H. Bleckmann (eds.). Springer, Berlin, Heidelberg, 2012, 119–134.

[22] E. Sarradj, C. Fritzsche, T. Geyer: Silent owl flight: Bird flyover noise measurements. AIAA Journal **49** (2011) 769–779.

[23] T. Geyer, E. Sarradj, C. Fritzsche: Silent owl flight: Experiments in the aeroacoustic wind tunnel. Fortschritte der Akustik – NAG / DAGA, Rotterdam, 2009.

[24] H. Butz, W. Biesel, W. Nachtigall: Einsatz spezieller Methoden der Photogrammetrie zur Untersuchung der Flügelgeometrie frei gleitfliegender Tauben. – In: BIONA-report 3. Akad. Wiss. Mainz. W. Nachtigall (ed.). G. Fischer, Stuttgart, New York, 1985, 123–138.

[25] H. Knappe, S. Wagner: Die aeroelastische Deformation von Vogelflügeln und ihr Einfluss auf die Profilpolaren. – In: BIONA-report 3. Akad. Wiss., Mainz. W. Nachtigall (ed.). G. Fischer, Stuttgart, New York, 25-44, 1985.

[26] F. V. Hutcheson, T. F. Brooks: Effects of angle of attack and velocity on trailing edge noise. 42nd AIA Aerospace Sciences Meeting, Reno, NV, 2004, AIAA paper 2004-1031.

[27] E. Sarradj, C. Fritzsche, T. Geyer, J. Giesler: Acoustic and aerodynamic design and characterization of a small-scale aeroacoustic wind tunnel. Applied Acoustics **70** (2009) 1073–1080.

[28] T. F. Brooks, M. A. Marcolini, D. S. Pope: Airfoil trailing edge flow measurements and comparison with theory incorporating open wind tunnel corrections. AIAA/NASA 9th Aeroacoustics Conference, Williamsburg, VA, 1984, AIAA paper 84-2266.

[29] T. F. Brooks, M. A. Marcolini, D. S. Pope: Airfoil trailing-edge flow measurements. AIAA Journal **24** (986) 1245–1251.

[30] R. K. Amiet: Refraction of sound by a shear layer. Journal of Sound and Vibration **58** (1978) 467–482.

[31] R. H. Schlinker, R. K. Amiet: Refraction and scattering of sound by a shear layer. NASA, Langley Research Center under Contract NAS1-15339, 1980.

[32] T. J. Mueller: Aeroacoustic measurements. Springer, Berlin, 2002.

[33] H. Brick, T. Kohrs, E. Sarradj, T. Geyer: Noise from high-speed trains: Experimental determination of the noise radiation of the pantograph. Forum Acusticum, Aalborg, 2011.

[34] T. Geyer, E. Sarradj, J. Giesler: Application of a beamforming technique to the measurement of airfoil leading edge noise. Advances in Acoustics and Vibration (2012) Article ID 905461. doi:10.1155/2012/905461.

[35] T. F. Brooks, W. M. Humphreys: A deconvolution approach for the mapping of acoustic sources (DAMAS) determined from phased microphone arrays. 10th AIAA/CEAS Aeroacoustics Conference, Manchester, England, 2004, AIAA paper 2004-2954.

[36] P. Sijtsma: CLEAN based on spatial source coherence. 13th AIAA/CEAS Aeroacoustics Conference, Rome, Italy, 2007, AIAA paper 2007-3436.

[37] E. Sarradj: A fast signal subspace approach for the determination of absolute levels from phased microphone array measurements. Journal of Sound and Vibration **329** (2010) 1553–1569.

[38] T. Geyer, E. Sarradj, C. Fritzsche: Measurement of the noise generation at the trailing edge of porous airfoils. Experiments in Fluids **48** (2010) 291–308.

[39] T. Mebs, W. Scherzinger: Die Eulen Europas: Biologie, Kennzeichen, Bestände. Kosmos Naturführer, 2000.

[40] T. Alerstam, M. Rosén, J. Bäckman, P. G. P. Ericson, O. Hellgren: Flight speeds among bird species: Allometric and phylogenetic effects. PLoS Biol **5** (2007) e197. doi:10.1371/journal.pbio.0050197.

[41] P. L. Lasagna, K. G. Mackall, J. Burcham, F. W., T. W. Putnam: Landing approach airframe noise measurements and analysis. NASA Technical Paper 1602, 1980.

[42] J. H. McDonald: Handbook of biological statistics. 2nd ed. Sparky House Publishing, Baltimore, MD, 2009.

[43] W. K. Blake: Mechanics of flow-induced sound and vibration. Volume I: General concepts and elementary sources. Academic Press, Inc., 1986.

[44] J. Jaworski, N. Peake: Aerodynamic noise from a poroelastic trailing edge with implications for the silent flight of owls. 18th AIAA/CEAS Aeroacoustics Conference, Colorado Springs, CO, 2012, AIAA paper 2012-2138.

[45] T. F. Brooks, D. S. Pope, M. A. Marcolini: Airfoil self-noise and prediction. NASA Reference Publication 1218, Hampton, 1989.

[46] W. S. Cleveland: Robust locally weighted regression and smoothing scatterplots. Journal of the American Statistical Association **74** (1979) 829–836.